RESEARCH ARTICLE

Accelerating Reliability Analysis of Deteriorated Simply Supported Concrete Beam with a Newly Developed Approach: MCS, FORM and ANN

Doha Al-Mosawe [a] , Luis Neves [b], John Owen [b]

[a] Civil Engineering Department, College of Engineering, Baghdad University; [b] Coates Building, School of Civil Engineering, University of Nottingham, University Park, Nottingham NG7 2RD, UK.

ARTICLE HISTORY
Compiled January 4, 2024

ABSTRACT
Reliability analysis methods are used to evaluate the safety of reinforced concrete structures by evaluating the limit state function $g(X_i)$. For implicit limit state function and nonlinear analysis , an advanced reliability analysis methods are needed. Monte Carlo simulation (MCS) can be used in this case however, as the number of input variables increases, the time required for MCS also increases, making it a time-consuming method especially for complex problems with implicit performance functions. In such cases, MCS-based FORM (First Order Reliability Method) and Artificial Neural Network-based FORM (ANN-FORM) have been proposed as alternatives. However, it's important to note that both MCS-FORM and ANN-FORM can also be time-consuming methods in their own right. MCS-FORM involves running multiple MCS, and the time required increases with problem complexity and desired precision. ANN-FORM, on the other hand, can be faster for repetitive reliability assessments, but the training phase can be computationally expensive, and accuracy depends on training data quality and quantity. To address this computational challenge and enhance the efficiency of reliability analysis, a novel method is proposed in this paper. This method leverages the capabilities of ABAQUS, in combination with MATLAB. The key objective of this proposed approach is to automate and streamline the repetitive tasks involved in reliability analysis, thereby significantly reducing the computational time required for such analyses. The method is based on the development of a custom ABAQUS Python script file, which interfaces with MATLAB. The script serves as a bridge between the finite element analysis capabilities of ABAQUS and the data processing and analysis capabilities of MATLAB. An illustrative example was considered to demonstrate the application of the proposed method. In this example, a deteriorated simply supported concrete beam with an implicit performance function was analyzed. The objective was to assess the reliability of the beam under the given conditions. To perform this reliability analysis, the two methods were employed: MCS-FORM and ANN-FORM. Both of these methods were implemented in conjunction with the newly developed approach that integrates ABAQUS and MATLAB. The results of this analysis were quite promising. Both MCS-FORM and ANN-FORM successfully estimated the reliability of the concrete beam, and they exhibited a high level of agreement in their assessments. This presented method demonstrates its suitability for the application of reliability analysis in scenarios such as the one presented. Its efficiency in automating repetitive tasks not only simplifies the analysis process but also facilitates the generation of multiple simulations. By doing so, it significantly minimizes the time and computational resources required for reliability assessments.

CONTACT D. M. Al-Mosawe. Email: doha.m@coeng.uobaghdad.edu.iq

KEYWORDS
Reliability analysis; corrosion; safety; new method; concrete; ABAQUS; MATLAB; ANN; MCS; FORM

1. Introduction

Reliability analysis is a method used to assess the safety and performance of structures, systems, and components under different conditions and uncertainties. It involves evaluating the probability of failure and estimating the associated risks, enabling engineers to design safer and more reliable structures. Generally, reliability analysis of technical components became an important issue during the Second World War. During this period significant problems were encountered especially in regard to the performance of electrical systems (Faber, 2005). Nowadays, reliability analysis has been developed for different applications and in a wide range of different industries such as the nuclear industry, chemical industry and building industry(Wang et al., 2022) and (Wang et al., 2023). Therefore, the application of reliability analysis received a worldwide acceptance from the engineering profession. Reliability analysis methods are used to assess the safety of reinforced concrete structures by evaluating a boundary called the limit state function $g(X_i)$. This function helps determine if a structure is safe or unsafe. It compares the strength or resistance of the structure to the effects of the applied load. The limit state function in many reliability analysis problems can be expressed explicitly and the First Order Reliability Method (FORM) can be used to estimate the safety of structure for explicit limit state function. However, for applications to realistic structures, e.g., when the structure behaves non-linearly due to cracking and crushing of concrete, yielding of reinforcement etc., the limit state function is expressed implicitly. The implicit limit state function is defined for the very complicated problems as long as an algorithm is available to compute the structural response (e.g. non-linear

finite element analysis). Finite element method is a tool that has become widely used for analysis of structures since its much more effective than other methods in dealing with the complexities of material nonlinearity and the 3D structural behaviour. Several research studies ((Ghabussi et al., 2020), (Wang et al., 2022), (Ghabussi et al., 2021) and (Li et al., 2023)) have utilized Finite Element Analysis (FEA), a powerful computational method in their work. FEA helps researchers simulate and analyze complex phenomena and giving a better understanding of how complex stuff works. In such cases (implicit limit state function), the derivative of $g(X_i)$, with respect to the random variables X, that is required in searching for the minimum distance point on the $g(X_i)$ is not available. Therefore, more advanced reliability methods are needed. Various strategies have been developed to address challenges related to implicit performance functions. One such method is the response surface method (RSM)(e.g., (Kim and Na, 1997), (Kmiecik and Soares, 2002) and (Teixeira and Guedes Soares, 2010)), which utilizes a polynomial function to approximate the unknown performance function. While RSM can provide a reasonably accurate estimate of failure probability, it may be time-consuming with a large number of random variables, and there is no assurance that the fitted surface closely matches the actual limit state in all regions. The other possible method of structural reliability analysis for implicit performance function is the sensitivity based analysis which has been detailed by Mahadevan and Haldar (2000). The sensitivity based analysis can be computed through a finite difference approach and perturbation method to compute the gradient of the $g(X_i)$ at each iteration during the search for the design point at the minimum distance (Mahadevan and Haldar, 2000). Although the sensitivity based analysis is more elegant and more efficient than RSM, it requires a specialized program that are not adaptable for practical applications (Wiśniewski, 2007).

The conventional Monte Carlo simulation (MCS) can also handle implicit performance functions $g(X_i)$ (Mahadevan and Haldar, 2000). Monte Carlo simulation is one of the methods that is used to calculate the probability of failure for any limit state function. This method is applicable when the limit state function is defined explicitly or implicitly. It can be applied to a variety of practical problems and can handle any type of probability distribution for random variables. Additionally, MCS can accurately compute the probability of failure and is easy to implement. However, this method can be computationally intensive and time-consuming, particularly when dealing with nonlinear systems with many input variables. According to Cardoso et al. (2008), the probability of failure for ultimate limit states typically falls within the range of 10^{-4} to 10^{-6}. To ensure a 95% confidence level with a 5% margin of error, a minimum of 1.6×10^7 to 1.6×10^9 analyses should be conducted. In such contexts, the computational cost and time required for MCS can become exceedingly burdensome, prompting the exploration of more efficient methodologies to expedite the reliability analysis process. Therefore, it can be clearly seen that the main issues in structural reliability assessment are the excessive computational cost as well as the accuracy and applicability of the method to complex structural problems involving implicit limit state function.

Two notable approaches that have emerged as potential alternatives to traditional MCS in this regard are Monte Carlo Simulation-based FORM (MCS-FORM) and Artificial Neural Network-based FORM (e.g., (Gomes and Awruch, 2004), (Elhewy et al., 2006), (Cardoso et al., 2008), (Papadrakakis et al., 1996) (Chojaczyk et al., 2015)) (ANN-FORM). These methods aim to strike a balance between computational efficiency and accuracy in reliability analysis. However, it's essential to acknowledge that even these advanced techniques, while offering advantages in specific scenarios, come with their own computational demands, which can be considered time-consuming relative to particular problem characteristics. MCS-FORM involves repeatedly running Monte Carlo simulations to estimate the probability of failure. Each simulation involves sampling random input variables and performing an analysis to evaluate the system's response. This process is repeated multiple times to obtain reliable statistics. The time required for this method increases significantly as the complexity of the problem and the desired level of precision grow. Moreover, when implicit performance functions are involved, the computational effort may further escalate.

ANN-FORM relies on artificial neural networks to approximate the system's behavior and estimate the probability of failure. While this approach can be faster than traditional MCS for repetitive reliability assessments, the initial phase of training the neural network can be computationally expensive, particularly for complex models and when a significant amount of training data is needed. Moreover, the accuracy of ANN-based FORM depends on the quality and quantity of the training data, which can pose challenges in certain situations.

In this paper, a novel approach is introduced aimed at increasing computational efficiency in case of implicit LSF. This methodology capitalizes on the functionalities of ABAQUS in conjunction with MATLAB. The principal objective of this innovative strategy is the automation and streamlining of iterative tasks substantial to reliability analysis leading to a substantial reduction in the computational time required for such analysis. The method is based on the development of a custom ABAQUS Python script file, which interfaces with MATLAB. The script serves as a bridge between the finite element analysis capabilities of ABAQUS and the data processing and analysis capabilities of MATLAB.

An illustrative example was considered to demonstrate the application of the proposed method. In this example, a deteriorated simply supported concrete beam with an implicit performance function was analyzed. The objective was to assess the reliability of the beam under the given conditions.

To perform this reliability analysis, two methods were employed: Monte Carlo Simulation-based FORM (MCS-FORM) and Artificial Neural Network-based FORM (ANN-FORM). Both of these methods were implemented in conjunction with the newly developed approach that integrates ABAQUS and MATLAB.

The results of this analysis were quite promising. Both MCS-FORM and ANN-FORM successfully estimated the reliability of the concrete beam, and they exhibited a high level of agreement in their assessments.

This presented method demonstrates its suitability for the application of reliability analysis in scenarios such as the one presented. Its efficiency in automating repetitive tasks not only simplifies the analysis process but also facilitates the generation of multiple simulations. By doing so, it significantly minimizes the time and computational resources required for reliability assessments. Overall, this approach showcases its practicality and effectiveness in addressing complex problems and can be a valuable tool for researchers and engineers seeking to enhance the efficiency of their reliability analysis endeavors.

2. Monte Carlo simulation

Monte Carlo simulation is one of the methods that is used to calculate the probability of failure for any limit state function. This method is applicable when the limit state function is defined explicitly or implicitly (when limit state function obtained from finite element analysis). In this approach, the most important task is to generate random samples of the random variables in order to simulate a large number of experiments. The generation of random numbers according to a specific distribution is the heart of Monte-Carlo simulation.
In structural reliability, a large number of samples are generated (simulated). For each sample outcome, the value of the limit state function is computed. The probability of failure after N simulations is estimated through:

$$P_f = \frac{n_f}{N} \tag{1}$$

where n_f is the number of simulations in which the failure is occurred ($g(X_i) < 0$) and N is the total number of simulations. By using a large number of simulations, the estimation of the probability of failure becomes close to the exact solution. This means that the estimation will converge to the correct answer when N is near ∞. Therefore, this method is less suitable for complex structures because large simulations are required to estimate the probability of failure and that requires many time consuming numerical calculations. The simulation of the N outcomes of the joint density function in Equation 1 is in principle simple and may be seen as consisting of two steps as shown in Figure 1. In the first step, a uniformly distributed random number, z_{ji}, is generated between 0 and 1 for each component of $\hat{x}_j$ using pseudo random number generator (PRNG). In the second step the outcomes of the pseudo random numbers

z_{ji} are transformed to outcomes of $\hat{x}_{ji}$ by:

$$x_{ji} = F_{X_i}^{-1}(z_{ji}) \tag{2}$$

where $F_{X_i}^{-1}()$ is the CDF for the random variable X_i.

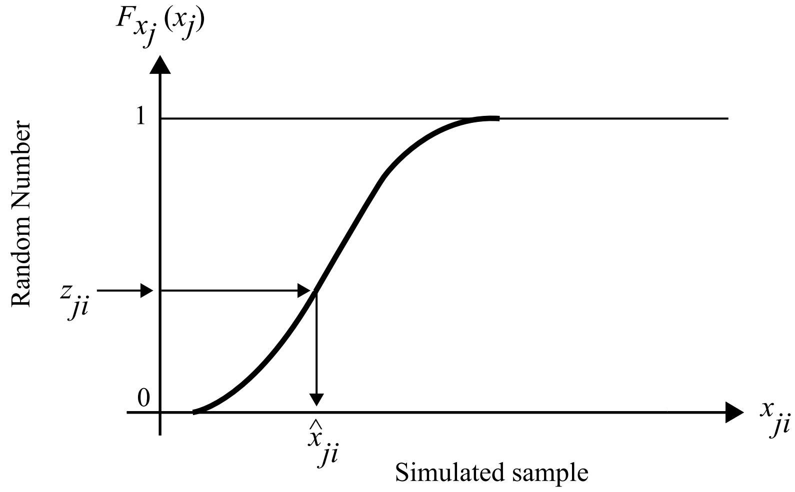

Figure 1. Principle for simulation of a random variable (Faber, 2005)

3. Artificial Neural Network method (ANN)

The ANN is a numerical algorithm introduced by McCulloch and Pitts (1943) by proposing a mathematical model to simulate neuron behaviour. The ANN model consists of multiple neurons linked together and situated in three or more layers: Input layer, Output layer and one or more hidden layers as shown in Figure 2.

Each neuron in the input layer will receive an input component of a signal vector that represents the input random variables $X_i = x_1, x_2, ...x_n$. After that, each random variable will be multiplied by a coefficient w_{mk} which reflecting the importance of the input channel k. The activation of neuron a_m is then calculated from Equation 3.

$$a_m = \sum_{k=1}^{n} w_{mk}.x_k + b_m \tag{3}$$

where b_m is the bias, which is a constant corrective term that allows having a non-negative activation a_m. The output signal s_m of neuron is the numerical value that results from the computation of an activation hyperbolic tangent sigmoid function $f(a_m)$, which is the common choice used for this purpose, and it can be calculated from Equation 4.

$$f(a_m) = s_m = \frac{2}{1 + e^{-2a_m}} - 1 \tag{4}$$

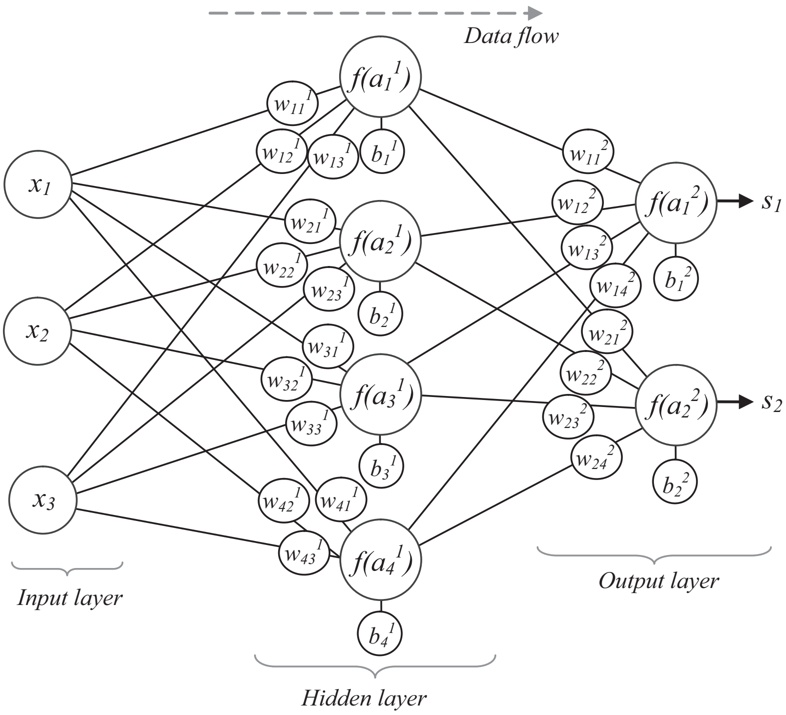

Figure 2. Multi-layer neural network (Chojaczyk et al., 2015)

The number of neurons on the input layer is equal to the number of input variables while the number of outputs it depends on the number of limit state functions that need to be approximated. The number of hidden layers and also the number of neurons in the hidden layers can be changed and there are no applicable general rules to choose them. Trial and error is usually used to find the suitable number of hidden layers.
The basic idea of ANN is to train a neural network model which can be used later on other values. The training of a network is an iterative process which consists of obtaining the unknown coefficients w_{mk} and b_m required to approximate the prescribed function. The most common training process, called *Back Propagation* training algorithm, consists in generating random values for the initial weights and biases and then adjusting values using a training algorithm to minimize the error between the predicted output produced by the ANN and the exact value of the function. Therefore, to perform this training test, a training data set, which includes input and target values, should be previously prepared. The iterative training algorithm performs an error minimization procedure that is repeated until the network outputs converges to the target value. The error is evaluated using the following equation (Mean Squared Error):

$$MSE = \frac{1}{N}\sum_{i=1}^{N}(t_i - s_i)^2 \tag{5}$$

where N is the number of training samples, s_i is the network output values and t_i is the target output.

Table 1. Deterministic values of beam geometry, material properties and load parameters

Parameter	Value	Units
Length (L)	9.5	m
Clear span (L_{cs})	9	m
Height (h)	0.4	m
Width (b)	0.25	m
Effective depth (d)	0.38	m
Compressive strength (f_{ck})	30	MPa
Steel yield strength (f_{yk})	500	MPa
Permanent load (g_k)	4	kN/m
Live load (q_k)	6	kN/m

4. Reliability analysis of a RC beam with implicit performance function

In this section, an example application of reliability analysis of a deteriorated RC beam with implicit performance function will be presented. Two methods have been used and compared:

- Combining MCS and FORM.
- ANN-based FORM.

4.1. Beam details and random variables

A simply supported reinforced concrete beam subjected to corrosion is considered in this study to assess the effect of corrosion and material strength variability on beam resistance and probability of failure over 90 years of the beam service life. The deterministic values of beam geometry, material properties and loads are listed in Table 1. Four reinforcement bars are embedded in the beam with diameter 16 mm as shown in Figure 3.
As the beam is tested under bending, the failure mode criteria is flexural and the ultimate limit state function occurs when the beam resistance is less than or equal to the bending action. Therefore, the limit state function is written as:

$$g(X_i) = \theta_R.M_R - \theta_E.M_S \tag{6}$$

where θ_R and θ_E are the resistance and load model uncertainties. M_R is the beam resistance moment that can be evaluated from ABAQUS. M_S is the beam action moment which can be calculated according to the applied dead and live load from the following equation:

$$M_S = wl^2/8 \tag{7}$$

where $w = g + q$. Then the limit state function is written as:

$$g(X_i) = \theta_R.M_R - (\frac{l^2}{8}(g+q)).\theta_E = 0 \tag{8}$$

In the reliability analysis, the compressive strength of concrete (f_c), the tensile strength of concrete (f_t), the yield stress of reinforcement steel (f_y), dead load (g), live load (q), the concrete modulus of elasticity (E_c), the resistance model uncertainty (θ_R) and the

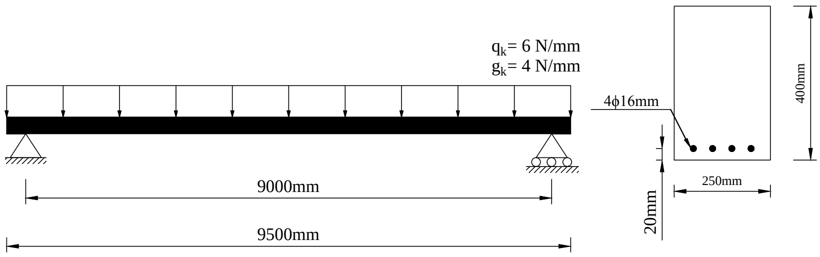

Figure 3. Simply supported RC beam section

Table 2. Statistical parameters of random variables for ultimate limit state analysis

Variables	Units	μ	σ	COV	Distribution	Source
Concrete compressive strength (f_c)	MPa	f_{cnom}	-	0.15	Lognormal	JCSS (2001)
Concrete tensile strength (f_t)	MPa	$0.3(f_c)^{2/3}$	-	0.2	Normal	Spaethe(1992) cited in Wiśniewski (2007)
Yield stress (f_y)	MPa	$S_{nom} + 2\sigma$	30	-	Normal	JCSS (2001)
Modulus of elasticity (E_c)	GPa	$22(0.1f_c)^{0.3}$	-	0.08	Normal	Eurocode-2 (2004)
Dead load (g)	kN/m	4	-	0.1	Normal	Nowak (1993)
Live load (q)	kN/m	6	-	0.4	Gumbel	Nowak (1993)
Load uncertainty (θ_E)	-	1	0.1	0.1	Lognormal	JCSS (2001)
Resistance uncertainty(θ_R)	-	1	0.15	0.15	Lognormal	JCSS (2001)

load model uncertainty (θ_E) are treated as random variables and their distribution, mean and standard deviation are presented in Table 2.
The analysis assumes deterministic values for corrosion rate ($i_{corr} = 3\mu.A/cm^2$) and pitting factor ($R = 4$) for simplicity. Furthermore, time to corrosion initiation (t_i) is assumed to be zero. According to the classification of corrosion rate in Middleton and Hogg (1998), $i_{corr} > 1.0$ represents a high corrosion rate typical of aggressive environments such as surfaces exposed to sea-spray.
The other relevant parameters for the mechanical properties for steel and concrete are included as implicit random variables.

4.2. 3D-nonlinear FE modelling

In the current paper, the nonlinear finite element method (FEM) is employed to characterize the model, mirroring the methodology established in (Al-Mosawe et al., 2022). This includes the modelling of material properties, application of loads, and the mesh size by performing a mesh sensitivity study. a nonlinear analysis has been performed to simulate the actual behavior of the beam. Figure 4 shows the 3D FE mesh for the nonlinear model for the RC simply supported beam. The model includes eight-node Solid elements (C3D8R) for concrete and Truss elements (T3D2) for reinforcement steel. The truss elements are embedded in the concrete element using embedded constraint, which means a perfect bond is assumed between concrete and steel. Elastic steel plattens are also added at the load positions and near the supports to avoid the stress concentration in the concrete. A tie constraint (surface based tie) is used to define the fully constrained contact behaviour between elastic strips and the concrete beam (Al-Mosawe et al., 2022). For the boundary conditions, the beam is simply supported and therefore, the movement is eliminated in x and y direction for the hinge and in y direction for the roller. A displacement control method is used to test the beams under four point bending.

Table 3. Concrete damage plasticity input parameters

Dilation angle (ψ)	Eccentricity (ε)	f_{b0}/f_{c0}	K_c	μ
31°	0.1	1.16	2/3	10^{-5}

This study conducts a mesh sensitivity analysis on a simply supported concrete beam to identify the optimal mesh size. While a coarse mesh enhances computational efficiency, it may yield inaccurate results, and a very fine mesh, though more accurate, can be excessively time-consuming. Consequently, mesh size is crucial in finite element analysis. Seven mesh sizes for the beam were assessed, and the ultimate load was compared against the number of elements. The results indicate a converged mesh when reducing size produces negligible differences. A decrease in elements (coarse mesh) corresponds to an increase in ultimate load due to inadequate representation of stress gradients. Thus, a coarse mesh hinders accurate structural assessment. This study determined that 9120 and 11232 elements yield close ultimate load values, with 9120 elements chosen for its reduced computational time

The behavior of concrete under tension and compression is simulated using the Concrete Damage Plasticity model (CDP) in ABAQUS. This model is versatile and can represent the characteristics of brittle materials like concrete, considering two main failure mechanisms: tensile cracking and compressive crushing. The reinforcement steel is represented by a simplified stress-strain curve with a Young's modulus of 200 GPa. The yield stress is set at 500 MPa, and the Poisson's ratio is 0.3, a standard value for steel. The damage parameters (d_c and d_t) are excluded from consideration within this investigation due to the absence of a cyclic relationship in the analytical framework. The analysis employs the CDP model incorporating the viscosity parameter (μ), the selection of which is informed by a sensitivity analysis detailed in Table 3. The incorporation of the viscosity parameter (μ) serves the purpose of mitigating convergence challenges encountered in ABAQUS analysis. Challenges in solution convergence may manifest as a consequence of heightened material non-linearity. Additionally, materials exhibiting softening characteristics are associated with negative tangent stiffness, thereby exacerbating convergence issues. Traditional finite element methodologies, such as stress increment reduction or an increase in the maximum number of steps within the Newton-Raphson method, may prove inadequate. Consequently, the CDP model integrates the viscosity parameter μ to facilitate plastic strain updates, with damage deduction facilitated through an additional relaxation time. The remaining parameters, including dilation angle ψ, eccentricity ϵ, yield surface factor K_c, and the ratio of initial biaxial compressive yield stress to initial uniaxial compressive yield stress (f_{b0}/f_{c0}), adhere to default values within the software, as outlined in Table 3. The beam is loaded under four point bending using a displacement control method by applying a target displacement value of 0.3 m. As vertical displacement increased, cracks due to bending were generated in the middle span of the beam as shown in Figure 5. The resistance moment at the middle section of the beam is calculated by finding the integration point stress for each element at the middle beam section and then these stresses are converted to moment by multiplying each element stress by its area and the distance from element center to the bottom of the beam.

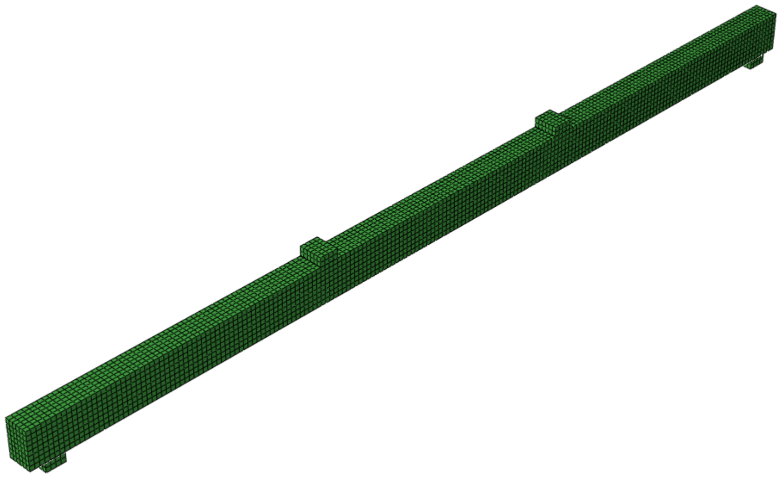

Figure 4. The three dimensional view of meshing the RC simply supported beam

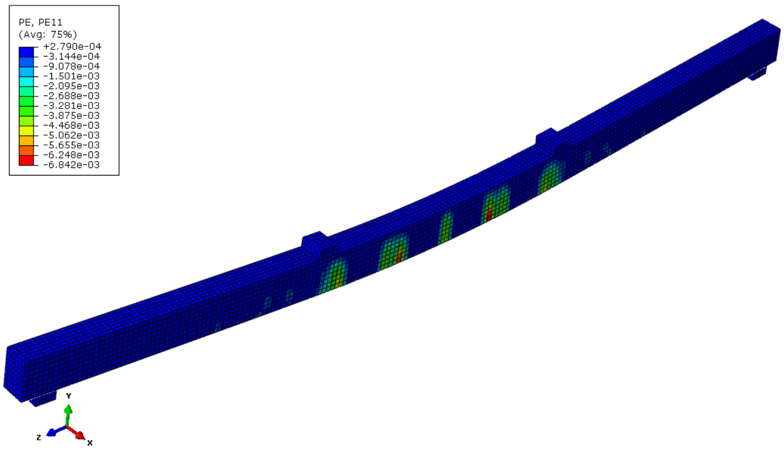

Figure 5. Beam cracks due to bending

4.3. Effect of pitting on reinforcement steel cross section

For simplicity, Val and Melchers (1997) assumed the pit form to be hemispherical as shown in Figure 6. The maximum pit depth at time t along a reinforcing bar is estimated from:

$$P(t) = 0.0116(t - t_i)i_{corr}R \tag{9}$$

where R is the pitting factor representing the extent of pitting corrosion as the ratio between the maximum and average corrosion penetration as follows:

$$R = P(t)/P_{av}(t) \tag{10}$$

$$P_{av}(t) = 0.0116 i_{corr}(t - t_i) \tag{11}$$

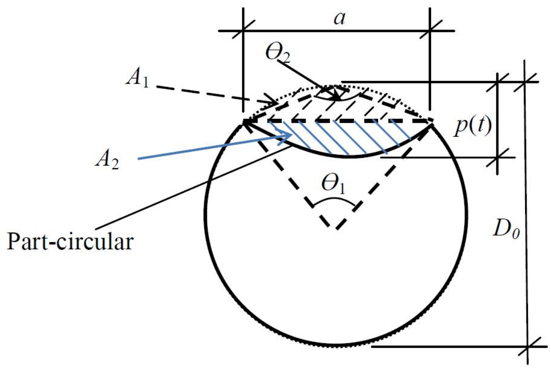

Figure 6. Non-uniform loss of reinforcement due to localized (pitting) corrosion (Val and Melchers, 1997)

The remaining area of the corroded steel at time t after pitting corrosion is then calculated as the following equations (Val and Melchers, 1997):

$$A_r(t) = \begin{cases} \frac{\pi . D_o^2}{4} - A_1 - A_2 & P(t) \le \frac{\sqrt{2}}{2} D_o \\ A_1 - A_2 & \frac{\sqrt{2}}{2} D_o < P(t) \le D_o \\ 0 & P(t) > D_o \end{cases} \tag{12}$$

where

$$A_1 = 0.5 \Big[\theta_1 . (\frac{D_o}{2})^2 - a . |\frac{D_o}{2} - \frac{P(t)^2}{D_o}| \Big] \tag{13a}$$

$$A_2 = 0.5 \Big[\theta_2 P(t)^2 - a . \frac{P(t)^2}{D_o} \Big] \tag{13b}$$

$$a = 2P(t) \sqrt{1 - [\frac{P(t)}{D_o}]^2} \tag{13c}$$

$$\theta_1 = 2\text{arcsin}(\frac{a}{D_o}) \quad and \quad \theta_2 = 2\text{arcsin}(\frac{a}{2P(t)}) \tag{13d}$$

4.4. Analysis procedure and results

After defining the limit state function and the relevant random variables, time dependent reliability analysis procedure according to Figure 7 has been applied. The procedure can be summarized in the following steps:

(1) By using MCS, a large number of samples for the resistance random variables (f_c, f_y, f_t and E_c) have been generated for each time interval.
(2) For each of the generated samples in step 1, the finite element beam model is prepared and analysed.
(3) The resistance moment is obtained after each finite element analysis for the beams in step 2.
(4) The statistical parameters of the resistance moment are found at each time interval.

(5) FORM method is used to evaluate the probability of failure (P_f).

Performing the steps listed above is quite complicated because they require a very long time to prepare the models and analyse them. For example, in this study MCS is used to generate 150 samples in step 1, which means 150 finite element models (for each time interval) need to be prepared and analysed in ABAQUS. So, if 10 years considered in time dependent reliability analysis, then 1500 finite element models need to be prepared and analysed. Doing that is impossible with the Graphical User Interface (GUI). Therefore, the ABAQUS Python script file is used in conjunction with MATLAB to reduce the time required for that, as will be explained in the next sections. Noting that, this is the first time that such method is used in structural reliability analysis to speed up the analysis via automating the processing. In conjunction with the above described method, the files have been prepared and submitted to the High Performance Computers (HPC) to complete several files at a time and to reduce the time required for each FEA.

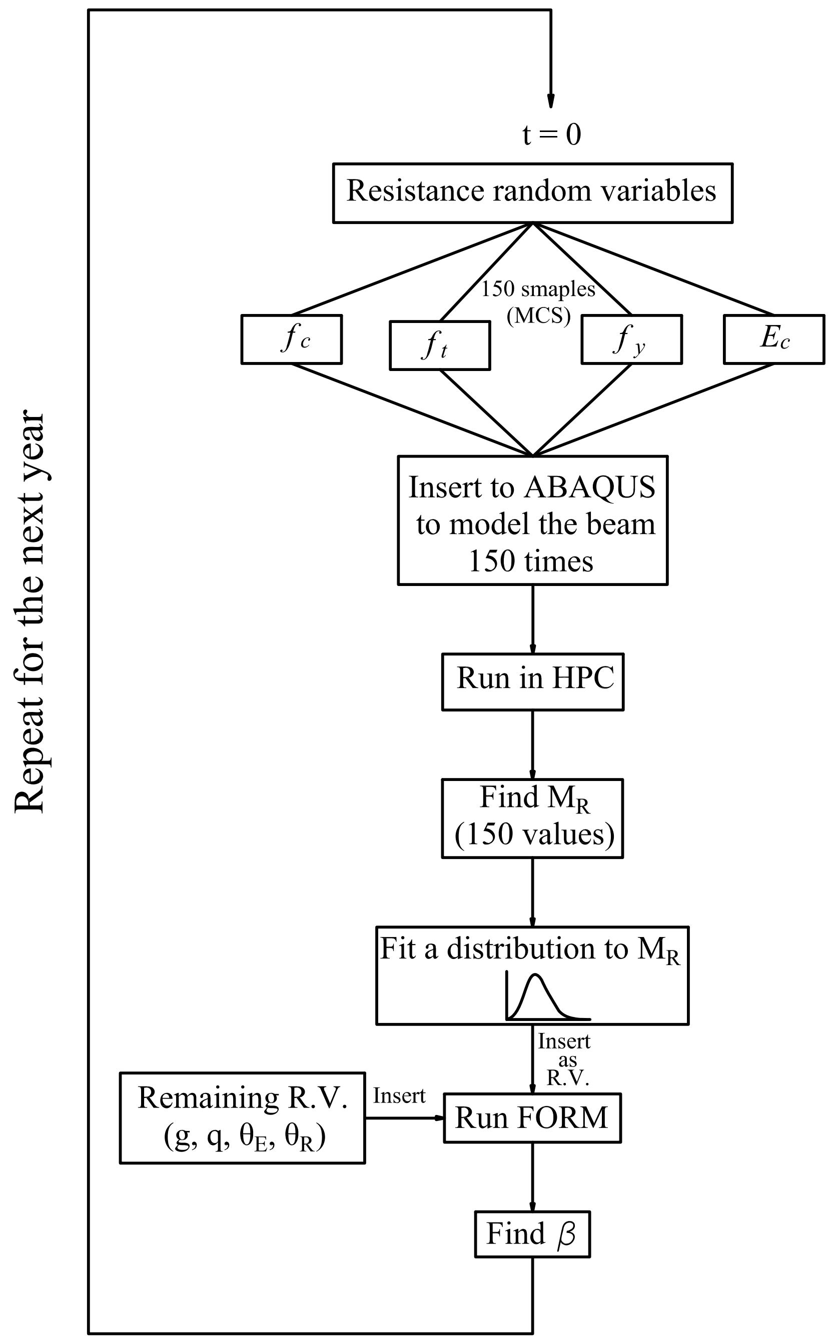

Figure 7. Reliability analysis procedure flowchart

4.4.1. ABAQUS Python script file

Python scripting language is a powerful tool used to communicate between modules like Graphical User Interface (GUI) in ABAQUS and ABAQUS/viewer. Python is embedded within ABAQUS software products. In some cases, using ABAQUS GUI to analyse a task can be considered as too time consuming or practically impossible, as is the case in this reliability analysis. For example, if a load is applied on a cantilever beam and the bending moment needs to be calculated as increasing the beam length then the beam should be recreated several times and if the model is complex then the sections, load, mesh and boundary conditions should be changed every time also. In this case, a Python script is a more efficient way to perform this task by considering e.g. length and load as a variables and rerunning the script in a loop for several times. Therefore, Python script is used in this study to automate the repetitive tasks that result from the uncertainty of material properties and geometry. In addition, using the script can help to extract information from large output databases.

To generate a Python script file for the model database (mdb) in ABAQUS, the following steps can be taken: First, create a finite element model using ABAQUS/GUI and complete the analysis. Save the model in a specific working directory. Then, open the journal file (*.jnl*) which records all the actions of model creation in ABAQUS and save it as a Python file (*.py*). This step generates the model database Python script file (*mdb.py*), which contains all the input data, such as model dimensions, material properties, mesh size, and more.

To generate the Python file for the output database (*odb.py*), you can follow these steps: Open the *.odb* file, which is created in the same directory, and specify the required results. Save the results in a *.rpt* file and exit. Finally, open the replay file (*.rpy*), which records all the actions of extracting the results from ABAQUS/viewer, and save it as a Python file (*.py*).

The *odb.py* file can be used to avoid the repetition of extracting the data from ABAQUS/viewer (*.odb* file). According to that, calculating the resistance moment in step 3 in Section 4.4 has been found one time, and then the steps of extracting these results are transformed to *odb.py* file.

4.4.2. ABAQUS and MATLAB connection

The two software applications ABAQUS and MATLAB can be connected together using Python file. The connection can help to automate the analysis, generate multiple simulations easily and minimize the time.
After preparing the *mdb.py* and the *odb.py* files, they were combined together in one file to accelerate the analysis. In MATLAB, the following steps are needed to complete the connection:

(1) Generate the resistance random variables samples, 150 samples for each year using MCS.
(2) Create a new Python file in terms of the resistance variables samples values generated in step 1.
(3) Execute the file prepared in step 2 in the model data base using execfile('filename.py').
(4) Run ABAQUS through MATLAB using **System** command. After this step, MATLAB will firstly read the *mdb.py* to create the model and secondly the *odb.py* to extract the results.

4.4.3. Resistance moment and beam capacity

The pitting corrosion is assumed to be distributed uniformly along the reinforcement bars. The pit configuration and its geometric model equations that are proposed by Val and Melchers (1997) is used in this study to predict the cross-sectional area of the pit (A_{pit}). According to this, the reinforcement corrosion is regarded through the steel bar area reduction as a function of time (Figure 8b) when the pit depth (Figure 8a) is generated over the reinforcement length. Figure 9 shows the deterioration in beam

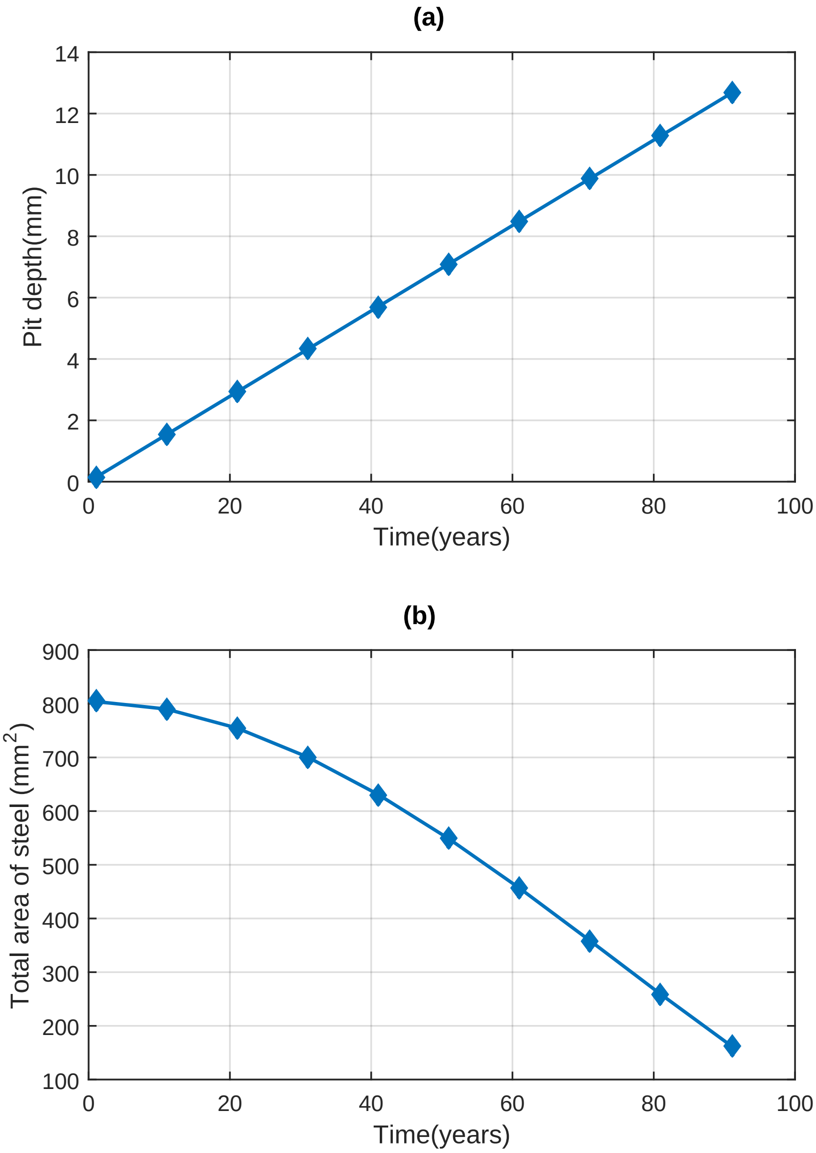

Figure 8. Model of steel corrosion (a) Increasing of pit depth with the time; (b) Reduction of the steel cross sectional area due to pitting corrosion

ultimate load capacity due to corrosion along the years. The ultimate load capacity of the beam corresponding to the corrosion loss over the years has been listed in Table 4. The table shows that the percentage reductions in ultimate capacity were in accordance with the findings of Malumbela et al. (2010), who found that for every 1% mass loss of steel, there was a corresponding 0.7% reduction in the ultimate capacity of the beam. Malumbela et al. (2010) performed an experimental test of corroded reinforced concrete beam to investigate the variation of mass loss of deformed steel bars along the corroded beam and its relationship with the residual capacity of RC beam. The result obtained in this paper are consistent to the results of Malumbela et al. (2010). This indicates that the finite element method used for modelling the simply supported beam works successfully.

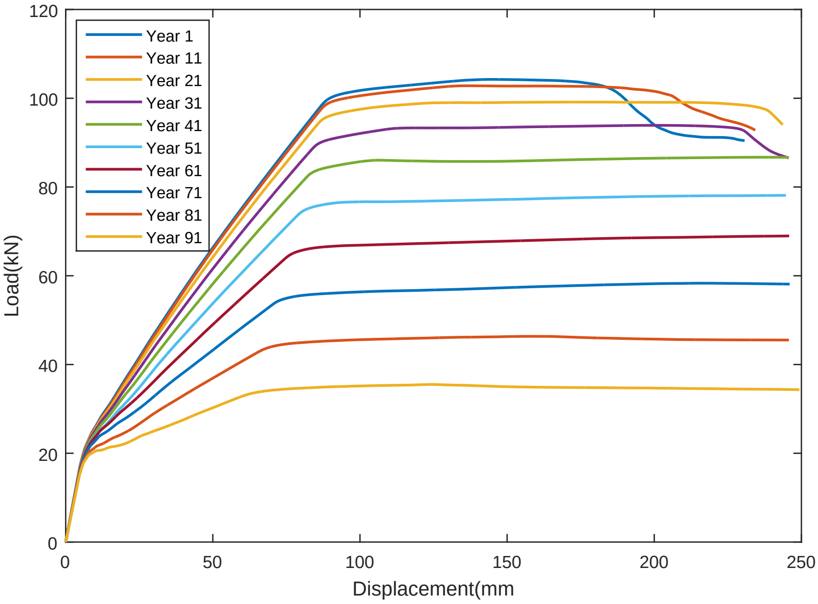

Figure 9. Load displacement curves at each year. The figure shows the deterioration of beam ultimate load capacity over the years due to corrosion

Table 4. Ultimate load capacity of the beam corresponding to different values of corrosion loss

Years	Corrosion loss	Ultimate load(kN)	Perecentage reduction in ultimate capacity
1	0	104.24	0
11	0.0175	102.81	0.013
21	0.0615	99.13	0.048
31	0.128	93.89	0.099
41	0.215	86.70	0.16
51	0.318	78.12	0.25
61	0.432	68.97	0.33
71	0.554	58.32	0.44
81	0.678	46.34	0.55
91	0.798	35.50	0.65

For the resistance moment, a lognormal distribution has been fitted and the mean value is also reduced as the corrosion progressed as shown in Figure 10. For the no corrosion case, the resistance moment histogram is shown in Figure 11, which shows that the mean value of the resistance moment is 176 kN.m with 9.1 kN.m standard deviation. Figure 12 demonstrates the effect of corrosion has on flexural strength capacity of the RC beam. The figure shows that with time the flexural strength of the beam decreases considerably. For example, after 51 years since corrosion initiation, the probability that the flexural resistance is less than 132 kN.m is around 50%. While for no corrosion case in the first year of the beam service life, the probability of getting a resistance moment less than 132 kN.m is zero. This indicates that corrosion has significant effect on the flexural resistance of the RC beams.

4.4.4. Probability of failure evaluation

After computing the resistance moment, the next step is to evaluate the probability of failure. As mentioned before, the probability of failure can be estimated using MCS by finding the ratio between the number of samples for which the limit state function

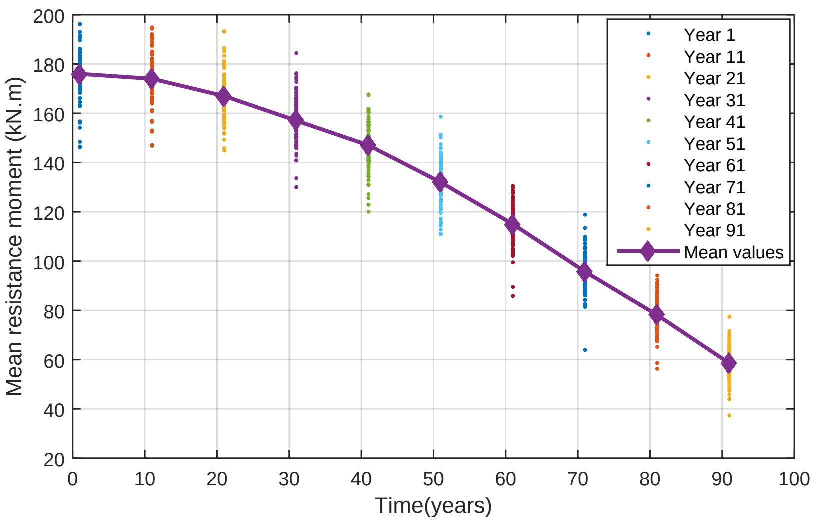

Figure 10. Reduction of the resistance moment mean value with the time due to corrosion

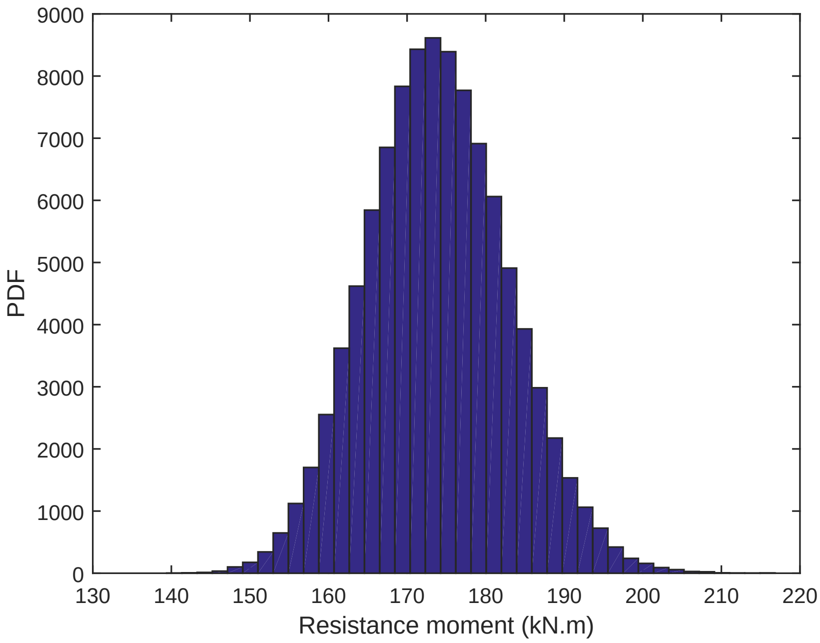

Figure 11. Histogram of flexural strength for no corrosion case (t = 0)

indicates failure to the total number of samples. However, the number of the generated samples in this study was small (150 samples) and accordingly, the direct estimation of the P_f will not be accurate and it might be underestimated by the results. Therefore, two methods have been used and compared in this study to estimate the P_f.
The first method is a combination between MCS and FORM analysis, while the second one which is proposed by Elhewy et al. (2006) is by training an ANN model and connect it with the reliability methods (FORM or MCS). The following sections explain and show the details and results of the two methods.

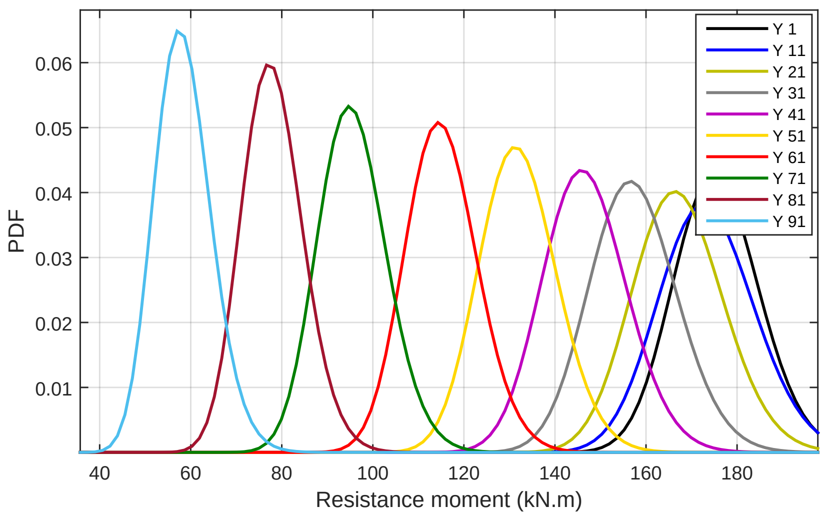

Figure 12. The effect of corrosion on the distribution of the beam resistance moment along the years

- **MCS with FORM**

  In this method, at each time interval, the values of the resistance moments are used in conjunction with FORM analysis to estimate the limit state function and the probability of failure. According to Equation 8, the random variables that are considered in FORM method are the resistance moment (M_R), resistance model uncertainty (θ_R), permanent load (g), the variable load (q) and the load model uncertainty (θ_E).

  The initial design points representing the mean values of each random variable were set for the first iteration. After solving a constrained optimization problem, when the reliability index β converged, the design points and the limit state function will be obtained. According to this approach, the reliability index and the probability of failure for each time interval are shown in Figure 13 a and b respectively. The results show that for the first year, when there was no corrosion, the reliability index was 3.45 which is lower than the target reliability index (β_T). The standard CEN (1990) recommends $\beta_T = 4.7$ for a one year reference period assuming no deterioration. That means the beam has not achieved the intended safety requirements since the reliability index is lower than the target one. This might be due to the absence of reinforcement at the top of the beam. Furthermore, assuming $i_{corr} = 3\mu.A/cm^2$ and $t_i = 0$ means a an aggressive environmental condition has been considered in this study. The reliability index decreased from 3.45 in the first year to more than half this value after 60 years of the beam service life, and that looks reasonable comparing with the remaining area of steel after 60 years, which is also reduced by half due to the aggressive environmental condition used in this study ($i_{corr} = 3\mu.A/cm^2$).

  A reliability analysis should be accompanied by a sensitivity analysis. Figure 14 shows the direction cosines at the design points of the random variables as a function of time. The direction cosines of each variables gives a measure of the impact that each random variable has on the estimated reliability index. The figure shows that the variable load (q) plays a fundamental role in the analysis with the largest sensitivity reaching -0.72 and exhibiting a reduction of its importance as the deterioration increase. This is followed by the resistance and load model uncertainties (θ_R and θ_E) with weights equal to 0.52 and -0.36 respectively. The influence of the resistance moment was insignificant for the first few years since the corrosion level was low, however, its importance increased considerably with the time as the corrosion level increase. The sensitivity coefficient of the resistance moment depends on the material properties and the corrosion rate.

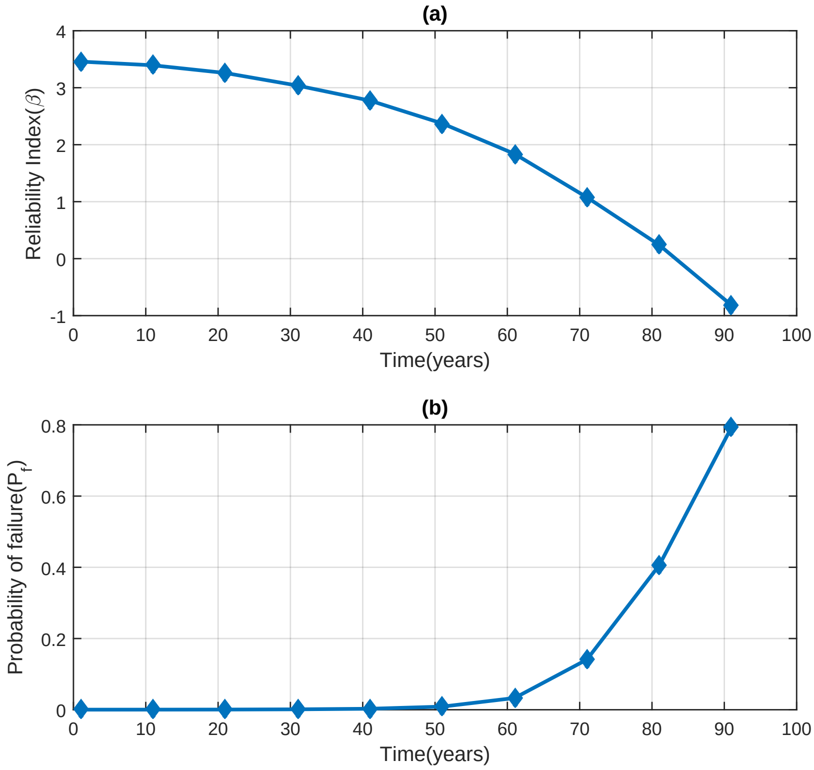

Figure 13. (a) Beam reliability indices reduction along the years. (b) Beam probability of failure increasing along the years

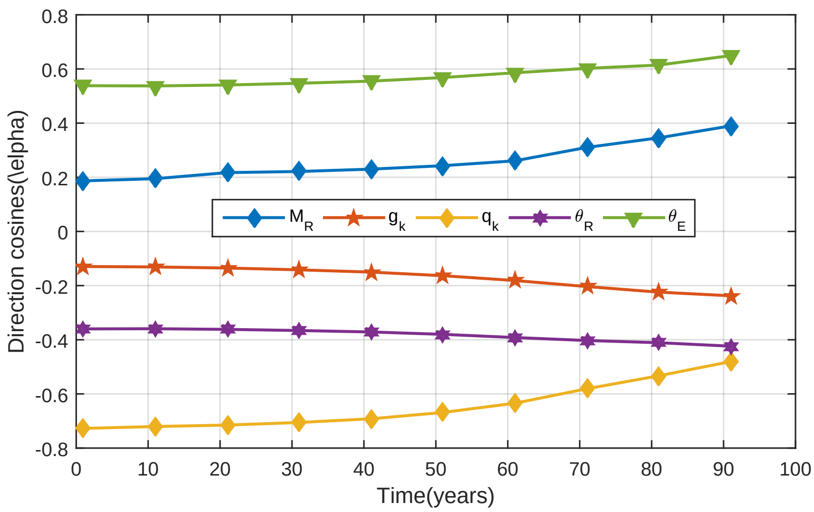

Figure 14. Direction cosines at design points as a function of time

- **ANN-based FORM**

  In this method, ANN models were prepared and used to predict the limit state function $g(X_i)$ and the probability of failure P_f that are obtained from the previous method. 10 ANN models (for each time interval) have been trained in this study. The ANN models are trained according to training data sets which include the input and the output (target) values. The training data sets considered in this study are represented by the 150 samples that are analysed using finite element analysis to get the limit state function.

  Ensuring the efficiency of the training process is contingent upon the careful selection of a representative sample set, a task of paramount importance. To optimize training efficacy, it is imperative to incorporate an adequate number of samples for each variable, facilitating the network's successful approximation of the Limit State Function (LSF) across its entire domain during recall. As the complexity of the reliability problem grows with an increased number of variables, the expansion of the sample set becomes a necessity. Furthermore, strategic dispersion of samples throughout the entire domain for each variable is vital for comprehensive learning. Therefore, the training data sets are prepared again by repeating the FEA for the beam with the same random variables, but increasing the standard deviation for each of them. That means, the variables that are considered in Table 2 are considered again with the same mean and twice their standard deviation (μ, 2σ).

  After the models have been trained, they will be connected with the reliability method (FORM) to predict the $g(X_i)$ and then P_f. The procedure that is used to tackle this method is as follows:

  - *Establish ANN model*

    To establish an ANN model two stages are needed: ANN model construction and ANN training and testing. In the first stage, the number of hidden layers and neurons number should be specified. Tarefder and Zaman (2005) stated that the accuracy of ANN depends on the network structure; however, there is no definite rule for choosing the hidden layers and the number of neurons at each layer. According to that, no rule has been depended in this study to select the number of hidden layers and neurons. Trial iterations were made to select the suitable number of layers and neurons for the hidden layer. To begin with, one layer with 3 and 5 neurons have been used, however, good results were not achieved as shown in Table 5. Then, ANN model was built again with using two hidden layers with 3 and 5 neurons at each layer respectively. The results were worth noticing that a greater number of layers and neurons can increase the accuracy of estimating the probability of failure as shown in Table 5. The table shows that using two hidden layers with 5 neurons at each of them resulted in closer value of reliability index to the one that is obtained from FORM method. According to that, the structure of ANN model used in this study consists of one input layer with 5 neurons (5 random variables: M_R, g, q, θ_E and θ_R), one output layer with one neuron ($g(X_i)$) and two hidden layers with 5 neurons at each layer, as shown in Figure 15.

    At the second stage (training and testing), the initial weight and biases are randomised. The models have been trained in this study using back propagation training algorithm which is a supervised learning algorithm that allows for training and adjusting the network by minimizing the error between the target and ANN output. At each network training, the data set

Table 5. Estimated reliability index (β)

Number of hidden layers	Number of neurons	β (NN) for year 1	β (FORM) for year 1	Difference(%)
1	3	3.63	3.45	4.7
1	5	3.50	3.45	1.2
2	3	3.55	3.45	2.6
2	5	3.45	3.45	2.90E-03

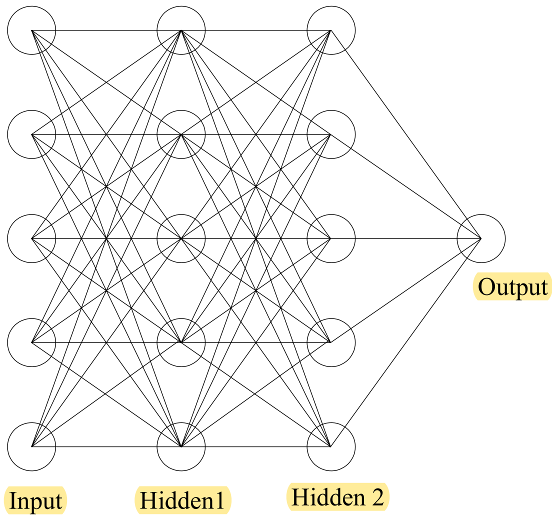

Figure 15. Structure of ANN

is processed many times as the connection weights and biases are adjusted by back propagation. At some desired level of accuracy, which can be evaluated by using an R^2 value and MSE, the training stops. R^2 represents the correlation factor between the target and the predicted values, while the MSE represents the difference between the desired and the predicted output. Therefore, a good prediction is achieved with higher value of R^2 and lower value of MSE.

In this study, 70% of the input and output data are used to train the model while 30% are used to test the model. Table 6 summarises the R^2 and the MSE for the ten trained ANN models. The best results are obtained with a very small MSE (near to zero) and a high R^2 (larger than 98%). According to this, the predicted limit state functions $g(X_i)$ by ANN are very close to the target or original values of $g(X_i)$ that are obtained from finite element analysis. Figure 16 shows a comparison between the predicted and the original values of $g(X_i)$.

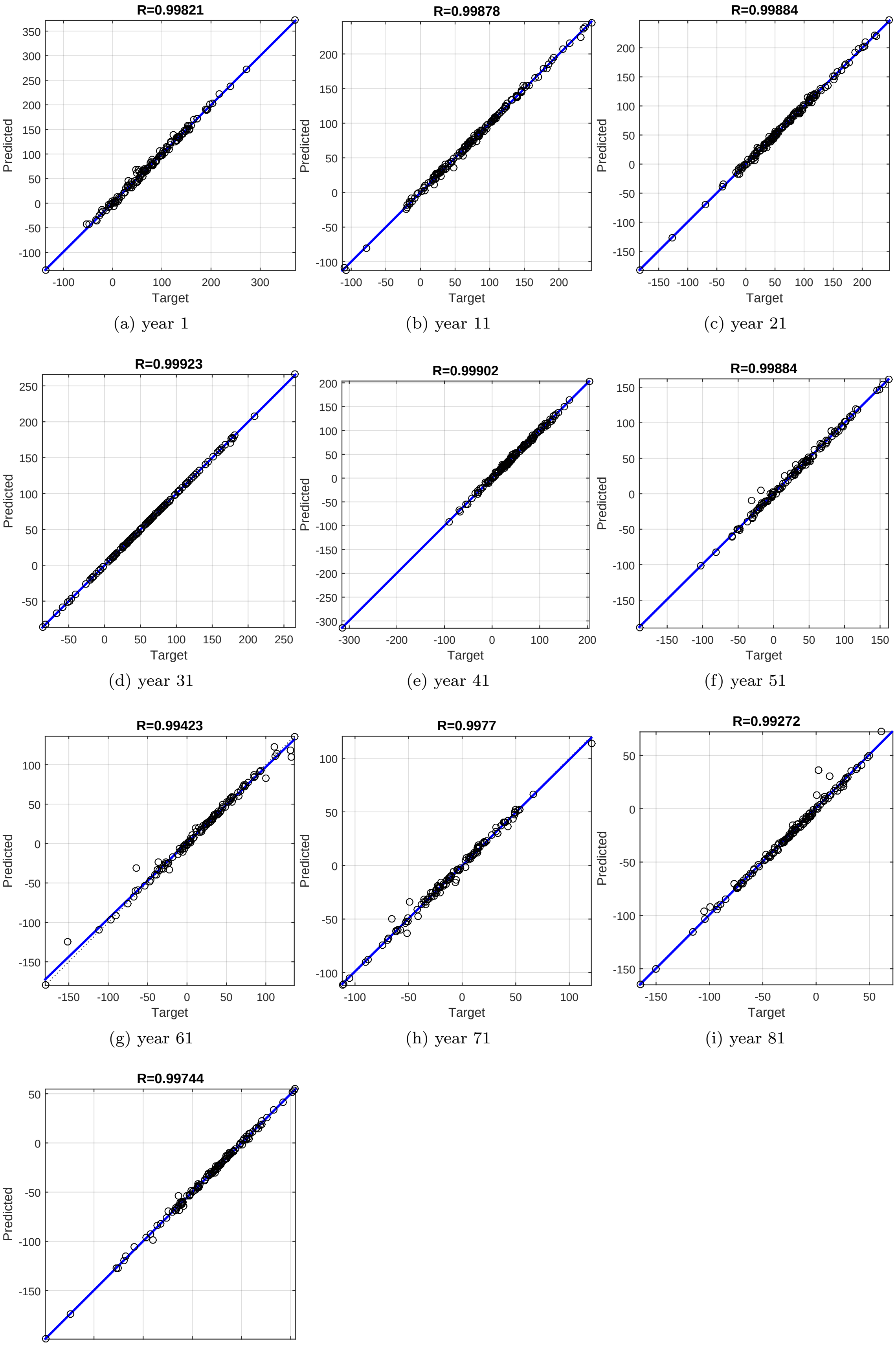

(a) year 1 (b) year 11 (c) year 21

(d) year 31 (e) year 41 (f) year 51

(g) year 61 (h) year 71 (i) year 81

(j) year 91

Figure 16. Predicted and target limit state function

Table 6. Performance of ANN model

Years	R^2-Training	R^2-Testing	R^2-All data	MSE
1	1	0.99539	0.998	2.66E-21
11	1	0.99595	0.99878	1.52E-21
21	1	0.99571	0.99884	1.91E-21
31	1	0.99674	0.99923	1.29E-21
41	1	0.99651	0.99902	1.21E-21
51	1	0.99616	0.99884	4.977E-22
61	1	0.98834	0.99423	1.09E-21
71	1	0.99338	0.9977	1.09E-21
81	1	0.98516	0.99272	1.09E-21
91	1	0.99045	0.99744	5.54E-22

- *Linking ANN to reliability method (FORM)*
  After all weights factors are fixed for the ANN models, they were linked to FORM method to estimate the probability of failure for each year and compare the results with that getting from the previous method (MCS and FORM). The simple way to link ANN with FORM is by setting the initial design points, the mean values of the random variables, at the first iteration. The trained ANN model will be called to estimate the limit state function at the given design point, then the calculation will be repeated until the reliability index converged. Figure 17 shows the comparison between the two methods. ANN-based FORM shows its efficiency to predict the probability of failure in which the results are very comparable between the two methods.

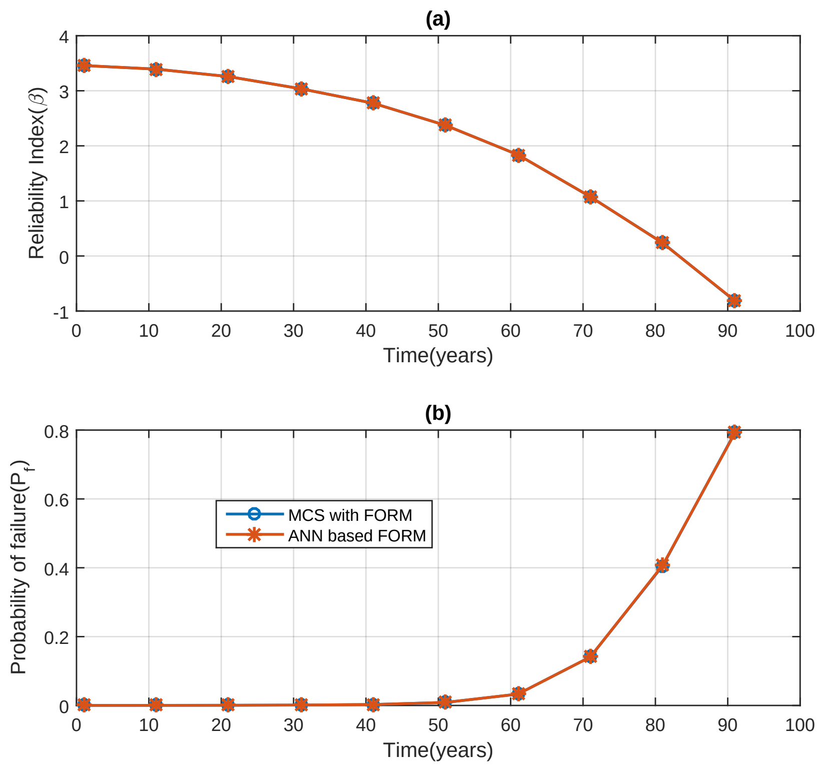

Figure 17. Comparison between the two methods: MCS with FORM and ANN-based FORM: (a) Reliability index (b) Probabilty of failure

5. Conclusion

In this paper, two methods: (a) combining MCS and FORM (b) ANN-based FORM have been applied on a simple example of RC beam subjected to corrosion. As the beam is modelled in ABAQUS and the nonlinear analysis is numerically costly, applying reliability analysis will be exhausted and a time consuming process. Therefore, by utilizing the ABAQUS and MATLAB connection (via a Python script file), an innovative combined process has been developed to enhance the efficiency of reliability analysis. The two methods have been successfully estimated the reliability of the beam and they show a good agreement with a very small difference (0.0029%) between them. The results also show that the effect of corrosion was very significant on the ultimate and flexural capacity of the beam. The percentage reduction in ultimate capacity were in accordance with the findings of Malumbela et al. (2010) in which they found that for every 1% maximum mass loss of steel there was a corresponding 0.7% reduction in the ultimate capacity of the beam. The computed reliability index is reduced sharply with the time due to the aggressive environmental condition considered in this study. The most important parameter for the analysis are traffic loads, followed by model uncertainties. This means that a correct definition of traffic load CoV is fundamental since it can drastically impact results. The weight of the resistance moment increased with the time as the corrosion increase. The method used in this chapter shows its applicability and efficiency to automate the repetitive tasks which can help to simplify the analysis, generate a multiple simulations easily and minimize the time.

This approach has the potential to offer a significant advantage in terms of computational time and resource utilization for researchers and engineers working on reliability problems in engineering and structural domains.

6. Acknowledgments

The main author is grateful for the financial supports from the Ministry of Higher Education and Scientific Research, Iraq.

References

Faber, M. H. (2005). Risk and safety in civil, surveying and environmental engineering. Technical report, Swiss Federal Institute of Technology.

Mahadevan, S. & Haldar, A. (2000). Probability, reliability and statistical method in engineering design.

Middleton, C. & Hogg, V. (1998). Review of deterioration models used to predict corrosion in reinforced concrete structures. Cambridge University.

McCulloch, W. S. & Pitts, W. (1943). A logical calculus of the ideas immanent in nervous activity. *The Bulletin of Mathematical Biophysics*, 5(4):115–133.

Chojaczyk, A., Teixeira, A., Neves, L. C., Cardoso, J., & Soares, C. G. (2015). Review and application of artificial neural networks models in reliability analysis of steel structures. *Structural Safety*, 52:78–89.

Gomes, H. M. & Awruch, A. M. (2004). Comparison of response surface and neural network with other methods for structural reliability analysis. *Structural safety*, 26(1):49–67.

Elhewy, A. H., Mesbahi, E., & Pu, Y. (2006). Reliability analysis of structures using neural network method. *Probabilistic Engineering Mechanics*, 21(1):44–53.

Review and application of artificial neural networks models in reliability analysis of steel structures. *Structural Safety*, 52:78–89.

Cardoso, J. B., de Almeida, J. R., Dias, J. M., & Coelho, P. G. (2008). Structural reliability analysis using monte carlo simulation and neural networks. *Advances in Engineering Software*, 39(6):505–513.

Malumbela, G., Alexander, M., & Moyo, P. (2010). Variation of steel loss and its effect on the ultimate flexural capacity of rc beams corroded and repaired under load. *Construction and Building Materials*, 24(6):1051–1059.

Tarefder, R. A. & Zaman, M. (2005). Design of neural networks for pavement rutting. In: *Applied Research in Uncertainty Modeling and Analysis*, pages 193–213. Springer.

JCSS (2001). Probabilistic model code. joint committee on structural safety. *URL: http://www.jcss.byg.dtu.dk/Probabilistic*.

Wiśniewski, D. F. (2007). *Safety Formats for the Assessment of Concrete Bridges*. PhD thesis, Universidade do Minho, Portugal.

Eurocode-2 (2004). *Eurocode 2: Design of Concrete Structures: Part 1-1: General Rules and Rules for Buildings*. British Standards Institution.

Nowak, A. S. (1993). Live load model for highway bridges. *Structural safety*, 13(1):53–66.

Val, D. V. & Melchers, R. E. (1997). Reliability of deteriorating rc slab bridges. *Journal of structural engineering*, 123(12):1638–1644.

CEN, E. (1990). Eurocode 2 Basis of Structural Design. European Committee for Standardization, 2002.

Papadrakakis, M. & Lagaros, N. D. (2002). Reliability-based structural optimization using neural networks and monte carlo simulation. *Computer methods in applied mechanics and engineering*, 191(32):3491–3507.

Papadrakakis, M., Papadopoulos, V., & Lagaros, N. D. (1996). Structural reliability analyis of elastic-plastic structures using neural networks and monte carlo simulation. *Computer methods in applied mechanics and engineering*, 136(1-2):145–163.

Kim, S.-H. & Na, S.-W. (1997). Response surface method using vector projected sampling points. *Structural safety*, 19(1):3–19.

Kmiecik, M. & Soares, C. G. (2002). Response surface approach to the probability distribution of the strength of compressed plates. *Marine Structures*, 15(2):139–156.

Teixeira, A. & Guedes Soares, C. (2010). Response surface reliability analysis of steel plates with random fields of corrosion. *Safety, reliability and risk of structures, infrastructures and engineering systems*, (2002):474–481.

Deng, J., Yue, Z., Tham, L., & Zhu, H. (2003). Pillar design by combining finite element methods, neural networks and reliability: a case study of the feng huangshan copper mine, china. *International Journal of Rock Mechanics and Mining Sciences*, 40(4):585–599.

Zhang, J. & Foschi, R. O. (2004). Performance-based design and seismic reliability analysis using designed experiments and neural networks. *Probabilistic engineering mechanics*, 19(3):259–267.

Chau, K.-W. (2007). Reliability and performance-based design by artificial neural network. *Advances in Engineering Software*, 38(3):145–149.

Wang, L., Zhou, Z., & Liu, J. (2022). Interval-based optimal trajectory tracking control method for manipulators with clearance considering time-dependent reliability constraints. *Aerospace Science and Technology*, 128:107745.

Wang, L., Zhao, Y., & Liu, J. (2023). A kriging-based decoupled non-probability reliability-based design optimization scheme for piezoelectric pid control systems. *Mechanical Systems and Signal Processing*, 203:110714.

Ghabussi, A., Marnani, J. A., & Rohanimanesh, M. S. (2020). Improving seismic performance of portal frame structures with steel curved dampers. In: *Structures*, volume 24, pages 27–40. Elsevier.

Wang, L., Zhao, X., Wu, Z., & Chen, W. (2022). Evidence theory-based reliability optimization for cross-scale topological structures with global stress, local displacement, and micro-manufacturing constraints. *Structural and Multidisciplinary Optimization*, 65(1):23.

Ghabussi, A., Marnani, J. A., & Rohanimanesh, M. S. (2021). Seismic performance assessment of a novel ductile steel braced frame equipped with steel curved damper. In: *Structures*, volume 31, pages 87–97. Elsevier.

Li, Z., Wang, L., & Lv, T. (2023). Additive manufacturing-oriented concurrent robust topology optimization considering size control. *International Journal of Mechanical Sciences*, 250:108269.

Al-Mosawe, D., Neves, L., & Owen, J. (2022). Reliability analysis of deteriorated post-tensioned concrete bridges: The case study of ynys-y-gwas bridge in uk. In: *Structures*, volume 41, pages 242–259. Elsevier.